罗涛, 王瀚林, 朱松柏, 等. 普通铅对 LA-ICP-MS 磷灰石 U-Pb 定年结果的影响及校正方法[J]. 岩矿测试, 2025, 44(1): 51−62. DOI: 10.15898/j.ykcs.202404070079.
LUO Tao, WANG Hanlin, ZHU Songbai, et al. Impacts of Common Lead on Apatite U-Pb Geochronology by LA-ICP-MS: Assessment and Correction Strategies[J]. Rock and Mineral Analysis, 2025, 44(1): 51−62. DOI: 10.15898/j.ykcs.202404070079.

普通铅对 LA-ICP-MS 磷灰石 U-Pb 定年结果的影响及校正方法

罗涛[1]，王瀚林[2]，朱松柏[2]，卿丽媛[1]，胡兆初[1]
(1. 中国地质大学 (武汉) 地质过程与矿产资源国家重点实验室，湖北 武汉 430074；
2. 中国石油塔里木油田公司克拉采油气管理区，新疆 库尔勒 841000)

摘要：磷灰石是火成岩、变质岩和沉积岩中广泛分布的含铀矿物，开展磷灰石 U-Pb 年代学研究对揭示岩浆演化过程、示踪溯源等方面具有重要意义。激光剥蚀电感耦合等离子体质谱法 (LA-ICP-MS) 是开展磷灰石 U-Pb 年龄微区分析的重要手段之一。当前，基体匹配磷灰石 U-Pb 定年矿物标样缺乏和标样中不可避免的普通铅是制约 LA-ICP-MS 高精度磷灰石 U-Pb 年龄分析的主要瓶颈。本文对比研究了标样中普通铅对 LA-ICP-MS 磷灰石 U-Pb 定年结果的影响，采用含普通铅的磷灰石 MAD 作外标直接开展 U-Pb 年龄校正，获得的被测样品年龄会产生显著的系统偏差 (最大约 6%)；采用^{207}Pb 法或 Tera-Wasserburg 图解法先校正标样中普通铅，再利用校正后的数据进行元素分馏和仪器漂移校正则可获得准确的磷灰石 U-Pb 年龄，与推荐值偏差在 2% 以内。另一方面，为消除标样中普通铅对分析结果的影响，本文还采用水蒸气辅助激光剥蚀方法，实现以 NIST612 玻璃作为外标准确分析磷灰石 U-Pb 年龄，解决了磷灰石 U-Pb 定年微区分析高质量标样缺乏的难题。本研究通过对标样中普通铅进行预校正或采用非基体匹配分析，建立了高精度 LA-ICP-MS 磷灰石 U-Pb 定年新方法，将促进磷灰石 U-Pb 年代学在地球科学研究中的应用。

关键词：激光剥蚀电感耦合等离子体质谱法；磷灰石；U-Pb 定年；普通铅校正；非基体匹配分析

要点：

(1) 使用含普通铅的磷灰石标样 MAD 作外标，直接校正样品产生 2.5%～6.0% 的系统偏差。

(2) 预先校正标样中普通铅 (^{207}Pb 法或 Tera-Wasserburg 图解法) 再进行样品 Pb/U 分馏校正可获得准确分析结果 (偏差低于 2.0%)。

(3) 采用水蒸气辅助激光剥蚀法，以玻璃 NIST612 非基体匹配分析磷灰石 MAD、Otter Lake 和 Durango 可获得准确年龄，有效地避免标样中普通铅对分析结果的影响。

中图分类号：O657.63；P597.3 **文献标识码：**A

磷灰石是各种地质环境中广泛存在的副矿物[1]，通常含有一定数量的铀 (几 μg/g 到数百 μg/g 以上)[2-3]，因此磷灰石 U-Pb 定年常用于限定成岩成矿和化石形成等重要地质作用时代[4-8]。激光剥蚀电感耦合等离子体质谱 (LA-ICP-MS) 因其样品制备简单、分析效率高、可提供微区原位信息等优点[9-11]，是开展副矿物 U-Pb 年龄微区分析的重要手段之一[4, 12-14]。对于 LA-ICP-MS 磷灰石 U-Pb 定年测定，Chew 等[12] 于 2011 年采用激光线扫描剥蚀法联合溶液校正建立 LA-ICP-MS 磷灰石 U-Pb 定年方法，此后该技术在磷灰石 U-Pb 年龄微区分析中应用广泛[15-19]。

由于磷灰石中铀含量通常较低[3]，采用激光微束分析时进样量少，其 Pb/U 分析精度是首要考虑的

收稿日期：2024−04−07；**修回日期：**2024−07−06；**接受日期：**2024−07−11；**网络出版日期：**2024−08−07
基金项目：国家自然科学基金项目 (42373032)；湖北省自然科学基金项目 (2024AFD372)
作者简介：罗涛，博士，副研究员，主要从事副矿物 U-Th-Pb 年代学和激光剥蚀电感耦合等离子体质谱机理研究。E-mail：luotao11@cug.edu.cn。

问题。Thomson 等[20]采用激光剥蚀联用 MC-ICP-MS 分析，分别用法拉第杯接收^{238}U、^{232}Th、^{208}Pb、^{207}Pb 和^{206}Pb，在激光剥蚀束斑 65μm 时获得的磷灰石标准样品 MAD 的^{206}Pb/^{238}U 单点分析精度为 4%～40%(2SD)。Chew 等[21]采用四极杆电感耦合等离子体质谱开展磷灰石 U-Pb 年龄分析，在剥蚀束斑 50μm 时获得的 Durango 磷灰石^{206}Pb/^{238}U 单点分析精度为 8%～10% (2SD)，而在束斑 130μm 时才达到满足激光分析要求的精度 (约 2%)。因此，开展激光微区磷灰石 U-Pb 定年分析时，评估仪器灵敏度对分析精度的影响是获得准确精密分析结果的基础。另一方面，磷灰石在结晶过程中矿物晶格中可能混入 Pb 元素，此类 Pb 不由 U、Th 等放射性衰变产生，即初始铅或普通铅[4]。不同成因的磷灰石普遍含有普通铅，已报道的用于磷灰石 U-Pb 定年微区分析的标准样品也均含有不同程度的普通铅[20-21]。U-Pb 定年分析标样需具有均匀的^{206}Pb/^{238}U 和^{207}Pb/^{206}Pb 比值，当磷灰石标样中有不同含量的普通铅时，标样实测的^{206}Pb/^{238}U 和^{207}Pb/^{206}Pb 比值是其放射性成因比值和不同含量普通铅的混合信息，若直接用于 Pb/U 分馏和仪器漂移校正，则会对磷灰石样品的定年结果和初始铅组成造成影响。前人开展磷灰石 U-Pb 定年分析时均采用基体匹配的磷灰石 MAD[20]作外标校正分析未知样品年龄，研究者多采用^{207}Pb 法先对 MAD 进行普通铅校正[16]。由于 MAD 标样普通铅含量低 (约 1% 的年龄不谐和)[20]，采用^{207}Pb 法可获得准确的分析结果，但该方法不适用于普通铅含量较高的标样分析。随着磷灰石原位 U-Pb 定年技术的发展和微区分析实验室数量的增加，低普通铅磷灰石 MAD 逐渐缺乏。为获得准确的激光微区 U-Pb 定年结果，因此需要对磷灰石标样中普通铅校正方法进行系统研究和开发非基体匹配分析方法。对当前特定副矿物 U-Pb 年龄微区分析高质量标样极度匮乏的问题，部分学者尝试开发了非基体匹配分析方法[4]。如以储量丰富、不含普通铅的锆石标样校正分析榍石[22]和金红石[23]等。Luo 等采用水蒸气辅助激光剥蚀方法实现以锆石或 NIST 玻璃作为外标分析榍石[13]、独居石[13]、磷钇矿[13]、氟碳铈矿[24]以及黑钨矿[25]等副矿物的 U-Th-Pb 年龄。采用非基体匹配分析方法，不仅可以有效地解决基体匹配标样缺乏的问题，也可一定程度地避免标样中普通铅组成对分析结果造成的偏差。

因此，针对当前激光微区磷灰石 U-Pb 定年分析时标样中普通铅影响分析结果准确度和精密度等问题，本文将定量评估分析灵敏度对磷灰石 U-Pb 定年分析精度的影响，对比研究磷灰石标样中普通铅组成对分析结果造成的偏差；尝试建立磷灰石非基体匹配分析方法以消除普通铅对分析结果的影响，建立了准确的高精度激光微区磷灰石 U-Pb 定年新方法。

1　实验部分

1.1　实验仪器

本实验在中国地质大学 (武汉) 地质过程与矿产资源国家重点实验室进行，采用 Agilent 7900 四极杆等离子体质谱仪 (Agilent Technology, Tokyo, Japan) 联合相干公司的 193nm 准分子纳秒激光 (GeoLas HD, MicroLas Göttingen, Germany)。详细的实验参数列于表 1。

表 1　LA-ICP-MS 磷灰石 U-Pb 定年实验仪器参数

Table 1　Instrumental parameters for LA-ICP-MS U-Pb dating of apatite.

LA 参数	GeoLas HD 193nm 准分子激光
波长	193nm
激光能量密度	10J/cm^2
剥蚀频率	5Hz
剥蚀时间	50s
背景时间	20s
He 流速	650mL/min
束斑直径	60～90μm
ICP-MS 参数	**Agilent 7900 型**
等离子体功率	1400W
样品气	0.86L/min
检测元素	^{29}Si, ^{42}Ca, ^{49}Ti, ^{51}V, ^{89}Y, ^{93}Nb, ^{139}La, ^{140}Ce, ^{141}Pr, ^{146}Nd, ^{147}Sm, ^{151}Eu, ^{157}Gd, ^{159}Tb, ^{163}Dy, ^{165}Ho, ^{166}Er, ^{169}Tm, ^{173}Yb, ^{175}Lu, ^{179}Hf, ^{181}Ta, ^{201}Hg, ^{204}Pb, ^{206}Pb, ^{207}Pb, ^{208}Pb, ^{232}Th, ^{238}U

1.2　实验样品和分析方法

MAD 磷灰石来自于马达加斯加的“1st Mine Discovery”。ID-TIMS 年龄测试出两个年龄 486±0.85Ma 和 474.25±0.41Ma，Th/U 值约为 15～30。MAD 磷灰石是目前激光微区磷灰石 U-Pb 年龄分析常用的外标[2,26]，本研究中基体匹配分析实验也采用 MAD 作为年龄校正标样。Durango 磷灰石产于墨西哥杜兰戈市的露天铁矿中，磷灰石的形成与长英质侵入体有关，产出于火山口的两个熔结凝灰岩之间[27]，同时结晶的四个单晶透长-歪长石的^{40}Ar-^{39}Ar 年龄为 31.44±0.18Ma (2SD)[27]。Durango

磷灰石由于年轻且 U 含量较低, Pb 同位素难以准确测定, 在测试中需要采用大束斑测量, 并固定初始铅组成, 或分析较大范围区域从而获得更为广泛的 Pb/U 组成分布[21]。Otter Lake 磷灰石产于加拿大魁北克省, 该地区的岩石经历了多期构造活动, 产自该地区的磷灰石样品通常呈深绿色-棕色长六角棱柱体, 对同一磷灰石晶体使用溶液法测试其铅同位素, 在$^{207}Pb/^{204}Pb$-$^{206}Pb/^{204}Pb$ 图解中获得的等时线年龄为 913±7Ma (2SD, MSWD=0.24), 该年龄作为 Otter Lake 磷灰石推荐年龄被广泛采用[21, 28]。为解决基体匹配标样缺乏的问题, 研究者们常采用美国国家标准与技术研究所 (NIST) 的合成玻璃 NIST610、NIST612 或 NIST614[29] 作为 U-Pb 年龄分析时的外标校正仪器分馏和信号漂移[13, 30-32], 本研究选用 U 含量与磷灰石较为相当的 NIST612 玻璃作为非基体匹配分析时的外部校正标样。数据处理采用 Iolite 软件[33] 和 Excel 程序, U-Pb 谐和图由 Isoplot R 软件绘制[34]。

2　结果与讨论

2.1　信号强度对分析精度的影响

U-Pb 定年的测试精度取决于 U 和 Pb 的信号强度, 而信号强度与样品中 U、Pb 的含量及进样量有关。由于含普通铅矿物的 U-Pb 年龄需要对其进行普通铅校正, 因此对于磷灰石 U-Pb 定年来说, 除了关注 Pb/U 的分析不确定度外, 还需注意 Pb/Pb 的分析不确定度。而 U-Pb 体系中的比值精度主要取决于低含量元素的信号强度。图 1 展示了在不同激光条件下同时测试磷灰石参考物质 MAD 和 Durango 获得 U-Pb 年龄的内部不确定度与 Pb 信号强度的关系。对于$^{206}Pb/^{238}U$, 当^{206}Pb 计数达到 6000cps 时, 其不确定度可以缩小到 2%; 当^{206}Pb 计数超过 6000cps 时, 其不确定度下降变缓, 超过 20000cps 时可以达到 ~ 1% 的不确定度。对于$^{207}Pb/^{206}Pb$, 其不确定度主要取决于含量更低的^{207}Pb 的信号强度, 因此其不确定度较$^{206}Pb/^{238}U$ 相比偏高。当 ^{207}Pb 计数为 ~ 600cps 时, 其不确定度可以达到 ~ 5%, 随后缓慢降低, 直到 ~ 2400cps 时达到 ~ 2% 的水平。从图 1 还可以看到, 对于年轻的样品 Durango, 由于其 Pb 含量过低, U-Pb 年龄的内部精度始终较低。

2.2　磷灰石 U-Pb 年龄基体匹配分析

副矿物 U-Pb 定年测试一般采用标样、样品间插分析以校正元素分馏和仪器漂移。而当外部校正标样中含一定程度普通铅时, 需要先对标样进行普通铅扣除, 使用经过校正后的 Pb/U 比值对未知样品进行校正。本研究对比了磷灰石 MAD 作外标时直接校正和选用不同方法进行普通铅校正后对待测样品分析结果的影响。

2.2.1　磷灰石 MAD 直接校正结果

如图 2 展示在不对标样 MAD 进行普通铅校正情况下, 直接用其校正监控样品的结果。对于 Otter Lake, 在不固定普通铅组成得到的 Tera-Wasserburg 谐和图交点年龄与推荐值的偏差在 1% 内, 但是初始铅组成与推荐值产生了较大偏差, 偏低 36%; 固定 Tera-Wasserburg 谐和图普通铅组成 ($^{207}Pb/^{206}Pb$=0.9, 由地球铅同位素演化模型[35] 确定), 交点年龄偏差为 2.5%。对于 Durango 磷灰石, 在不固定初始铅组成 ($^{207}Pb/^{206}Pb$=0.84) 得到的 Tera-Wasserburg 谐和图交点年龄偏差达到了 30%, 初始铅组成与推荐值产生了较大偏差, 偏低 60%; 固定 Tera-Wasserburg 谐

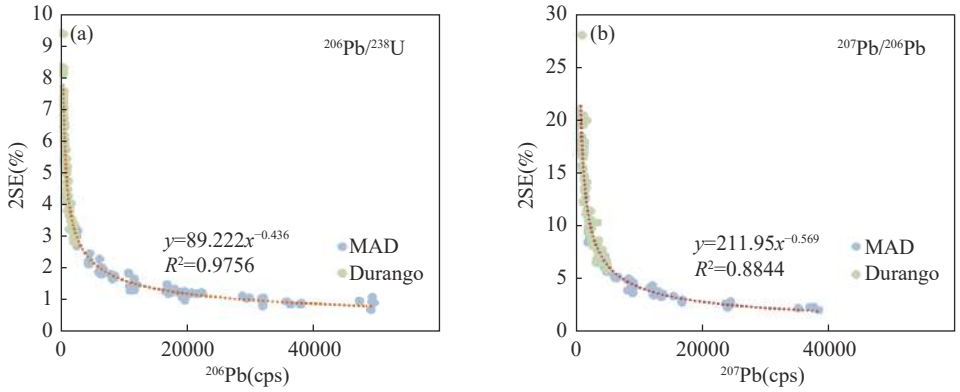

(a)$^{206}Pb/^{238}U$ 年龄; (b) $^{207}Pb/^{206}Pb$ 年龄。

图1　$^{206}Pb/^{238}U$ 和$^{207}Pb/^{206}Pb$ 年龄精度随 Pb 信号强度的变化

Fig. 1　The precision of $^{206}Pb/^{238}U$ and $^{207}Pb/^{206}Pb$ ages varing with Pb signal intensity: (a) $^{206}Pb/^{238}U$ age; (b) $^{207}Pb/^{206}Pb$ age.

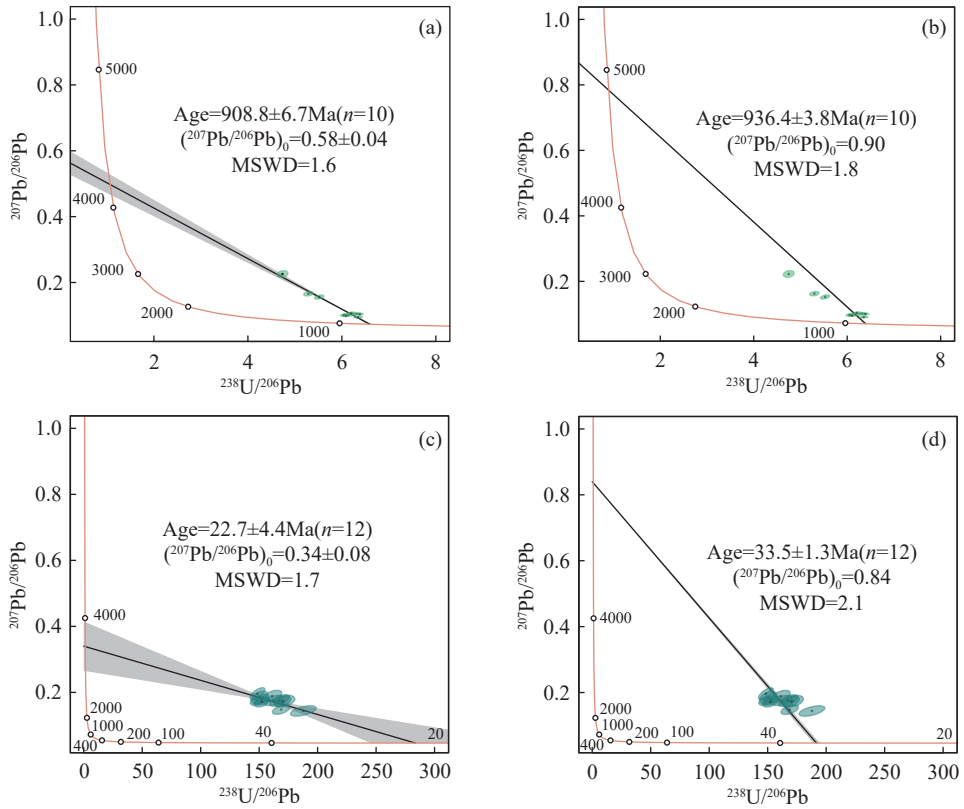

(a) 磷灰石 Otter Lake，不固定初始铅同位素；(b) 磷灰石 Otter Lake，固定初始铅同位素；(c) 磷灰石 Durango，不固定初始铅同位素；(d) 磷灰石 Durango，固定初始铅同位素。

图2　使用磷灰石 MAD 作为外标直接校正获得的磷灰石样品 U-Pb 年龄

Fig. 2　U-Pb ages results obtained by calibrating with apatite MAD as the external standard: (a) Apatite Otter Lake, without anchored initial Pb isotopic composition; (b) Apatite Otter Lake, with anchored initial Pb isotopic composition; (c) Apatite Durango, without anchored initial Pb isotopic composition; (d) Apatite Durango, with anchored initial Pb isotopic composition.

和图普通铅组成，交点年龄偏差为 6%。研究结果表明使用含普通铅的磷灰石标样作为外标时，若不对其进行普通铅校正，最终获得的被测样品年龄和初始铅组成均会产生较大的系统偏差。

2.2.2　^{207}Pb 法普通铅校正结果

对含普通铅的标准样品，常需对标样进行普通铅校正，再采用经过校正后的各标样对未知样品进行元素分馏和仪器漂移校正[4]。本研究选用^{207}Pb 法先对磷灰石标样 MAD 进行校正[4]，其校正原理和操作步骤简述如下。用于分馏校正的磷灰石标样中含普通铅时，需先对标样中普通铅进行校正。

若采用^{207}Pb 法校正：(a) 先对每个标样测试点的 U、Pb 信号扣除背景；(b) 对每个标样测试点进行普通铅校正，计算公式如下所示。

$$^{206}Pb_r = {}^{206}Pb_m \times (1 - f_{206}) \quad (1)$$

$$^{207}Pb_r = {}^{207}Pb_m - {}^{206}Pb_m \times \left(^{207}Pb/^{206}Pb\right)_c \times f_{206} \quad (2)$$

$$f_{206} = \frac{(^{207}Pb/^{206}Pb)_m - (^{207}Pb^*/^{206}Pb^*)}{(^{207}Pb/^{206}Pb)_c - (^{207}Pb^*/^{206}Pb^*)} \quad (3)$$

式中：$^{206}Pb_r$ 为普通铅校正后的瞬时 ^{206}Pb 信号；$^{206}Pb_m$ 为测试的瞬时^{206}Pb 信号；$^{207}Pb_r$ 为普通铅校正后的瞬时^{207}Pb 信号；$^{207}Pb_m$ 为测试的瞬时^{207}Pb 信号；$(^{207}Pb/^{206}Pb)_m$ 为测试的^{207}Pb/^{206}Pb 比值 ($^{207}Pb/^{206}Pb)_c$ 为初始的^{207}Pb/^{206}Pb 比值。

(c) 经过普通铅校正后的各标样点再用于 Pb/U 分馏校正。具体校正步骤可在 Iolite 软件[33]中的 VizualAge UComPbine 功能实现。

图 3 展示了 MAD 经过普通铅校正后分析磷灰石 Otter Lake 和 Durango 的结果。对于 Otter Lake，在不固定普通铅组成得到的 Tera-Wasserburg 谐和图交点年龄偏差为−1.5%，普通铅组成与推荐值的偏差为−10%；固定 Tera-Wasserburg 谐和图普通铅组成，交点年龄偏小于 1%。对于 Durango 磷灰石，在不固定普通铅组成得到的 Tera-Wasserburg 谐和图交点年龄偏差为−31.4%，普通铅组成与推荐值偏差为

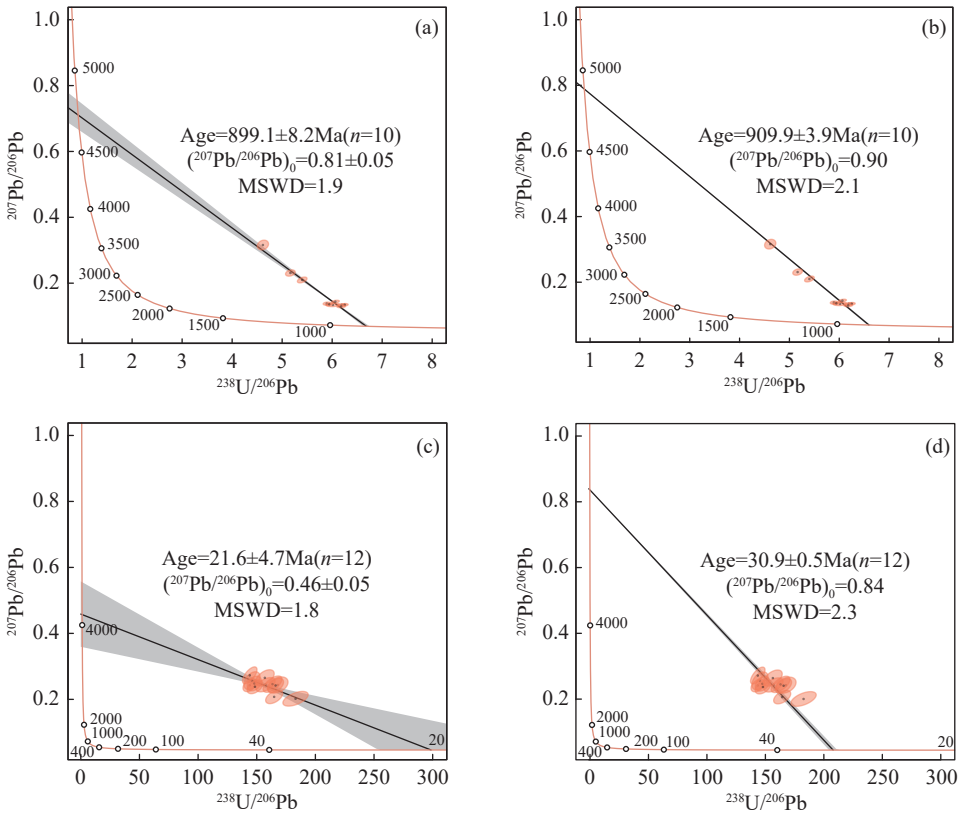

(a) 磷灰石 Otter Lake，不固定初始铅同位素；(b) 磷灰石 Otter Lake，固定初始铅同位素；(c) 磷灰石 Durango，不固定初始铅同位素；(d) 磷灰石 Durango，固定初始铅同位素。

图3　使用^{207}Pb 法校正 MAD 普通铅后获得的磷灰石样品的 U-Pb 年龄

Fig. 3　U-Pb age results obtained after prior correction for common Pb in MAD with ^{207}Pb method: (a) Apatite Otter Lake, without anchored initial Pb isotopic composition; (b) Apatite Otter Lake, with anchored initial Pb isotopic composition; (c) Apatite Durango, without anchored initial Pb isotopic composition; (d) Apatite Durango, with anchored initial Pb isotopic composition.

−45.4%; 固定 Tera-Wasserburg 谐和图普通铅组成, 交点年龄偏差为−1.7%。磷灰石标样 MAD 先经过普通铅校正, 后校正获得的磷灰石 Otter Lake 和 Durango 年龄与其推荐值相比偏差均在±2% 以内, 达到了目前国际上激光剥蚀微区分析磷灰石 U-Pb 定年的普遍水平[16, 21, 36-37]。

2.2.3　Tera-Wasserburg 图解法普通铅校正结果

^{207}Pb 法假定样品的^{206}Pb/^{238}U 和^{207}Pb/^{235}U 年龄谐和, 其数学校正原理可在 Tera-Wasserburg 图解上清晰呈现[4]。因此有学者采用标样测试点构筑的不一致线在 Tera-Wasserburg 图解下交点与其推荐值之比进行未知样品的分馏校正[4, 32]。其操作步骤为: ①分别计算出由所有测试点构筑的不一致线与 X 轴的交点; ②计算经过标样推荐年龄的不一致线与 X 轴的交点, 两交点比值即为 Pb/U 分馏校正系数; ③将该系数乘以待测样品的 Pb/U 比值便得到待测样品经过校正后的 Pb/U 比值, 而未知样品的^{207}Pb/^{206}Pb 比值则由 Pb 同位素组成均匀的标样 (如 NIST 玻璃) 直接校正获得。

图 4 展示了使用 Tera-Wasserburg 图下交点法校正得到的结果。将未经普通铅校正的磷灰石 MAD 测试点固定上交点于 0.87(由地球铅同位素演化模型[35]确定), 其不一致线与 X 轴的交点为 18.33, 将 MAD 推荐年龄 (475Ma)[20] 也投入图中, 得到经过推荐年龄的不一致线与 X 轴的交点为 14.14 (图 4a), 将两者的比值 (0.79) 校正到磷灰石 Otter Lake 和 Durango 各测试点 (图 4 中 b, c), 最终得到的 Tera-Wasserburg 谐和图交点年龄分别为 929.0±7.1 Ma (2σ, MSWD=1.2) 和 29.3±0.5Ma(2σ, MSWD=1.0), 与其各自推荐值偏差分别为 1.7% 和 6.6%。磷灰石 Durango 的结果呈现较大偏差, 可能是由于其普通铅含量较高, 分析获得的 Pb/U 比值不够分散, 因此其下交点年龄出现较大偏差。这也说明为获得准确的分析结果, 采用 Tera-Wasserburg 图解校正法时, 分

析样品需有较大范围的 Pb/U 比值。

2.3　磷灰石 U-Pb 年龄非基体匹配分析

水蒸气辅助激光剥蚀法现已广泛应用于榍石、独居石、磷钇矿和氟碳铈矿等副矿物 U-Th-Pb 年龄的非基体匹配分析[4, 13]。为避免标样中普通铅对分析结果造成的影响，本研究也采用水蒸气辅助激光剥蚀方法，以 NIST612 玻璃作为外标，校正磷灰石 MAD、Otter Lake 和 Durango 的 U-Pb 年龄。水蒸气引入方法在本团队以往研究中已有详细介绍[4, 13, 24]，本研究通过在剥蚀池前引入 4.0mg/min 水蒸气，选用 NIST612 玻璃作为外标直接校正磷灰石标样，分析结果如图 5 所示。磷灰石 MAD、Otter Lake 和 Durango 在 Tera-Wasserburg 图解下交点年龄分别为 474.7±2.7Ma (2σ, MSWD=1.6)、934.8±2.1Ma(2σ, MSWD=2.1) 和 31.2±1.2Ma (2σ, MSWD=1.6)，与其推荐值均在误差范围内一致。

2.4　不同分析方法结果对比

本研究为获得准确的磷灰石 U-Pb 年龄，分别采

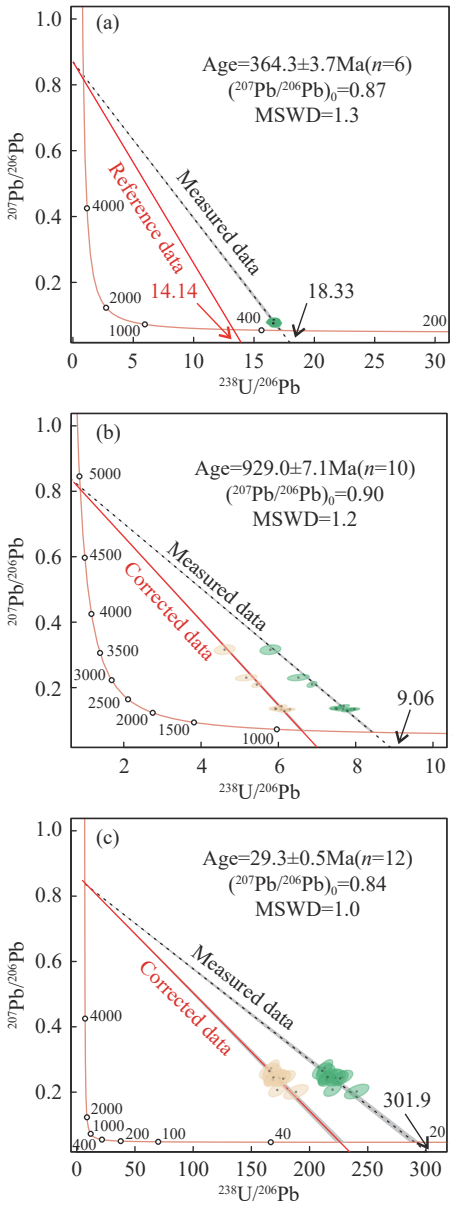

(a) MAD; (b) Otter Lake; (c) Durango。

图4　Tera-Wasserburg 图解法校正获得磷灰石 U-Pb 年龄

Fig. 4　U-Pb ages of apatite obtained by Tera-Wasserburg concordia correction method: (a) MAD; (b) Otter Lake; (c) Durango.

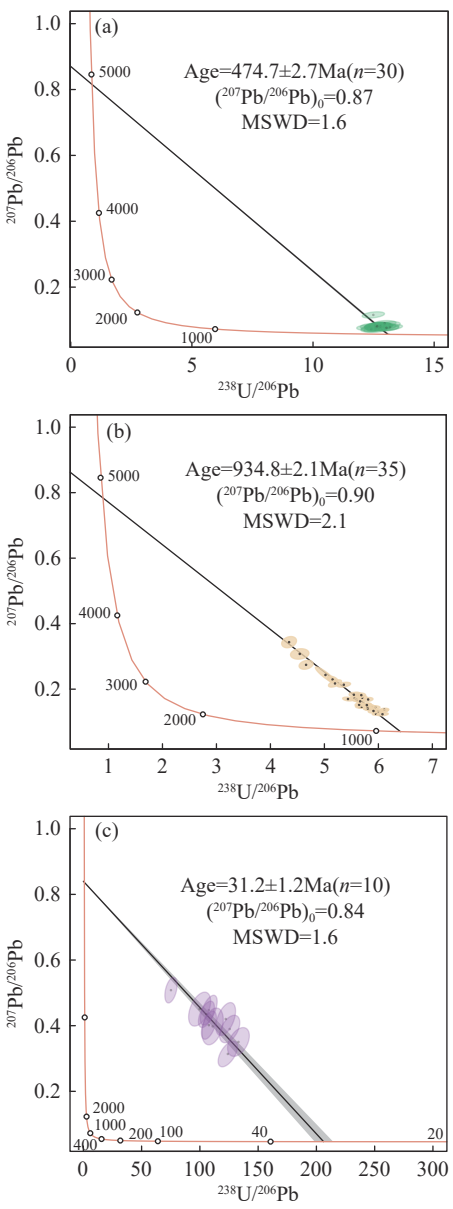

(b) MAD; (b) Otter Lake; (c) Durango。

图5　以 NIST612 玻璃作为外标分析获得的磷灰石 U-Pb 年龄

Fig. 5　U-Pb ages of apatite obtained by using NIST612 glass as the external standard: (a) MAD; (b) Otter Lake; (c) Durango.

用磷灰石 MAD 和 NIST612 玻璃作为外标校正分析, 并对比了^{207}Pb 法和 Tera-Wasserburg 图解法对 MAD 标样中普通铅的校正结果 (表 2)。由于测试所得磷灰石 Otter Lake 和 Durango 的 Pb/U 比值较为集中, 且含较高程度普通铅, 此处仅列出固定普通铅时计算的年龄结果。磷灰石 MAD 作为外标直接校正时, 固定初始铅组成, 获得的 Otter Lake 下交点年龄与推荐值的偏差为 2.5%; Durango 磷灰石的下交点年龄与推荐值的偏差为 6%。使用^{207}Pb 法先对磷灰石标样 MAD 进行普通铅校正, 获得的 Otter Lake 和 Durango 的交点年龄与其推荐值的偏差分别为 0.03% 和 1.7%。采用 Tera-Wasserburg 图解法校正 MAD 中普通铅后获得的 Otter Lake 和 Durango 的交点年龄与其推荐值的偏差分别为 1.7% 和 6.6%, 其中 Durango 的结果呈现较大偏差, 可能因为分析点的 Pb/U 比值不够分散, 获得的 Tera-Wasserburg 图解下交点有较大偏离导致。以 NIST612 玻璃作为外标, 测试的磷灰石 MAD、Otter Lake 和 Durango 在 Tera-Wasserburg 图解下交点年龄分别为 474.7±2.7Ma(2σ, MSWD=1.6)、934.8±2.1Ma(2σ, MSWD=2.1) 和 31.2±1.2Ma(2σ, MSWD=1.6), 与其推荐值的偏差分别为 0.1%、2.3% 和 0.8%。虽然本研究中采用^{207}Pb 法和 Tera-Wasserburg 图解法都可以获得磷灰石 Otter Lake 和 Durango 准确的 U-Pb 年龄, 但在标样普通铅含量较高时, 采用^{207}Pb 法可能会存在过校正或校正不足的情况, 造成样品年龄偏差, 因此^{207}Pb 法适用于普通铅含量较低的标样校正; 而 Tera-Wasserburg 图解法需要测试标样的 Pb/U 比值分散程度较大, 构筑不一致线以获得准确的下交点, 因此 Tera-Wasserburg 图解法适用于标样 Pb/U 比值分散程度较大的情况, 应用范围广, 但操作较为复杂。采用水蒸气辅助激光剥蚀非基体匹配分析, 可避免标样中普通铅对分析结果的影响, 同时有效地克服磷灰石标样匮乏的瓶颈。

表 2　不同测量条件下获得的磷灰石 Tera-Wasserburg 谐和图下交点年龄与推荐值的偏差

Table 2　Deviations of Tera-Wasserburg values and recommended values for apatite U-Pb age obtained under different measurement conditions.

激光条件	外标	普通铅校正方法	分析样品	Tera-Wasserburg 谐和图下交点年龄与推荐值的偏差 (%)
60μm, 5Hz	MAD	无普通铅校正	Otter Lake Durango	2.5 6.0
60μm, 5Hz	MAD	^{207}Pb	Otter Lake Durango	0.03 1.7
60μm, 5Hz	MAD	Tera-Wasserburg 图解法	Otter Lake Durango	1.7 6.6
60μm, 5Hz	NIST612	无普通铅校正	MAD Otter Lake Durango	0.1 2.3 0.8

3　结论

系统评价了磷灰石标样中不可避免的普通铅组成对 U-Pb 定年分析结果的影响。采用磷灰石 MAD 作外标直接开展 U-Pb 年龄分析, 获得的被测样品年龄和初始铅组成均会产生显著的系统偏差 (6%)。分别采用^{207}Pb 法或 Tera-Wasserburg 图解法校正标样中普通铅, 再使用校正后结果进行元素分馏和仪器漂移校正, 最终获得准确的磷灰石 U-Pb 年龄, 测试值与推荐值的相对偏差在 2% 误差范围内。此外, 为完全消除标样中普通铅的影响, 本文通过在剥蚀池前引入 4.0mg/min 水蒸气, 实现了以 NIST612 玻璃作为外标校正磷灰石 MAD、Otter Lake 和 Durango 的 U-Pb 年龄。该方法简单有效, 可以缓解激光微区磷灰石 U-Pb 定年分析高质量标样匮乏的难题。

本文通过建立基体匹配和非基体匹配分析方法, 有效地解决了磷灰石 U-Pb 定年分析时标样中普通铅对分析结果的影响, 成功实现磷灰石 U-Pb 定年准确分析。未来研究仍需加强低普通铅磷灰石 U-Pb 定年标准样品研制, 促进非基体匹配磷灰石 U-Pb 定年方法的推广, 为磷灰石 U-Pb 年代学在地球科学研究中的应用提供支撑。

致谢: 感谢审稿人对本文提出的宝贵修改建议。

Impacts of Common Lead on Apatite U-Pb Geochronology by LA-ICP-MS: Assessment and Correction Strategies

LUO Tao[1], *WANG Hanlin*[2], *ZHU Songbai*[2], *QING Liyuan*[1], *HU Zhaochu*[1]
(1. State Key Laboratory of Geological Processes and Mineral Resources, China University of Geosciences (Wuhan), Wuhan 430074, China;
2. PetroChina Tarim Oilfield Company, Korla 841000, China)

HIGHLIGHTS

(1) A systematic bias of 2.5% to 6.0% is observed when using the common lead-containing apatite standard MAD as an external standard for direct U-Pb calibration.

(2) Accurate results (with bias below 2.0%) can be obtained by correcting for common lead in the standard (using the ^{207}Pb method or Tera-Wasserburg diagram method) prior to performing Pb/U elemental fractionation correction.

(3) Accurate U-Pb ages of apatite reference materials of MAD, Otter Lake, and Durango can be obtained through calibration against non-matrix-matched NIST612 glass using a water vapor-assisted laser ablation method, effectively mitigating the influence of common lead in standards on the analytical results.

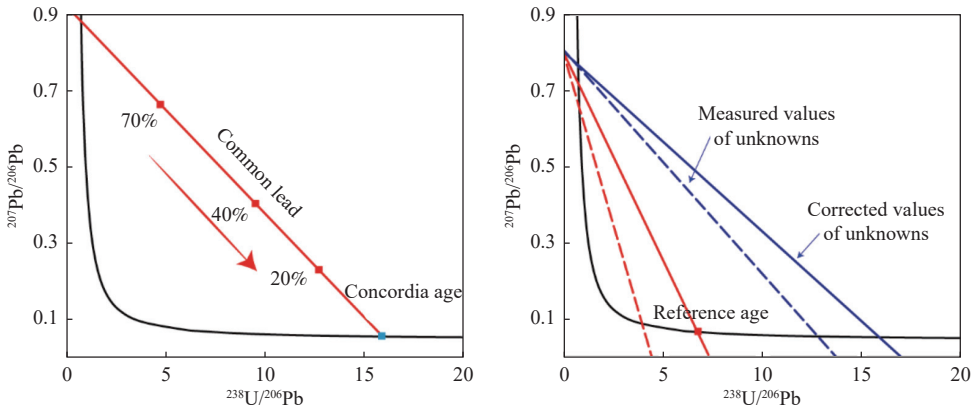

ABSTRACT: Apatite is a widespread U-bearing mineral in igneous, metamorphic, and sedimentary rocks. U-Pb geochronology of apatite can provide significant information for constraining magmatic evolution processes and tracing provenance. Laser ablation inductively coupled plasma-mass spectrometry (LA-ICP-MS) is a crucial technique for *in situ* U-Pb age analysis of apatite. However, the lack of suitable matrix-matched apatite reference materials and the inevitable presence of common lead in reference materials are major obstacles restricting high-precision determination of apatite U-Pb ages. This study investigates the impact of common lead on LA-ICP-MS apatite U-Pb dating results. The significant systematic biases (6%−30%) in both measured lower intercept ages and initial lead compositions are observed when calibrating against MAD apatite without common lead correction. However, accurate apatite U-Pb ages (within 2% systematic bias) can be obtained by correcting for common lead in MAD using the ^{207}Pb method or Tera-Wasserburg plot method prior to Pb/U fractionation calibration. Furthermore, a vapor-assisted laser ablation method is employed in conjunction with NIST612 glass as an external standard to accurately analyze apatite U-Pb ages. This non-matrix matched method eliminates the need to consider the influence of common lead in the reference materials. Novel high-precision LA-ICP-MS apatite U-Pb dating methods are

established with both matrix-matched and non-matrix-matched analyses, which greatly promote the application of apatite U-Pb geochronology in Earth science. The BRIEF REPORT is available for this paper at http://www.ykcs.ac.cn/en/article/doi/10.15898/j.ykcs.202404070079.

KEY WORDS: laser ablation inductively coupled plasma-mass spectrometry; apatite; U-Pb dating; common lead correction; non-matrix-matched analysis

BRIEF REPORT

Significance: Apatite is a ubiquitous accessory mineral occurring in diverse geological environments[1]. It typically contains U ranging from a few to several hundred ppm or more[2-3]. Consequently, apatite U-Pb dating is widely employed to constrain the timing of significant geological processes, including diagenesis, mineralization, and fossil formation[4-8]. Laser ablation inductively coupled plasma-mass spectrometry (LA-ICP-MS) is one of the important techniques for conducting *in situ* U-Pb age analysis of accessory minerals. Matrix-matched standards are crucial for obtaining accurate results in LA-ICP-MS U-Pb geochronology. However, apatite from diverse geological origins typically incorporates common lead, and the standards reported for *in situ* U-Pb geochronology of apatite likewise contain variable amounts of common lead. The measured Pb/U ratios are a mixture of radiogenic and common lead components when the apatite standards contain variable amounts of common lead. In previous apatite U-Pb geochronology studies, the ^{207}Pb method was commonly employed to correct for common lead in MAD standards, which contain minimal common lead (approximately 1% age discordance). However, this approach is unsuitable for analyzing standards with higher common lead contents. As *in situ* U-Pb dating techniques for apatite continue to advance and the number of microanalysis laboratories expands, the availability of apatite MAD standards with low common lead content is diminishing. To obtain accurate and precise LA-ICP-MS apatite U-Pb results, different common lead correction methods (^{207}Pb method or Tera-Wasserburg plot method) are performed to the apatite standard prior to Pb/U elemental fractionation correction in this study. Moreover, a water vapor-assisted method is proposed to determine accurate apatite U-Pb ages with NIST612 glass as the external standard. This non-matrix-matched analytical approach alleviates the lack of apatite U-Pb dating standards and effectively mitigates the impact of common lead in apatite standards on analytical results.

Methods: Experiments were performed with Agilent7900 quadrupole inductively coupled plasma-mass spectrometer (Agilent Technologies, Tokyo, Japan) coupled with a Coherent 193nm excimer nanosecond laser ablation system (Geolas HD, MicroLas Göttingen, Germany). Detailed experimental parameters are presented in Table 1. Apatite reference materials MAD, Durango, Otter Lake, and NIST612 glass were analyzed for U-Pb dating. For matrix-matched apatite U-Pb dating analysis, MAD was used as an external standard and Durango, and Otter Lake served as monitors to evaluate data accuracy. To obtain accurate and precise apatite U-Pb results, different common lead correction methods (^{207}Pb method or Tera-Wasserburg plot method) were performed to the MAD standard prior to Pb/U elemental fractionation correction. The calibration procedures for the ^{207}Pb method were as follows: (1) Subtract the background from the U and Pb signals for each measured MAD; (2) Perform common lead correction for each measured MAD; (3) Use the common lead-corrected MAD samples for Pb/U fractionation correction. These specific correction steps can be implemented using the VizualAge UComPbine function in the Iolite software. The principle of the Tera-Wasserburg plot method is based on the Tera-Wasserburg concordia diagram. The processes are as follows: (1) Calculate the intersection point of the discordia line constructed from all measured MAD with the X-axis of the Tera-Wasserburg concordia diagram; (2) Calculate the intersection point of the discordia line passing through the recommended age of the MAD standard with the X-axis. The ratio of these two intersection points is the Pb/U fractionation correction factor; (3) Correct the Pb/U ratios of unknown samples using the fractionation correction factor. The ^{207}Pb/^{206}Pb ratios of the unknown samples were directly corrected

using a standard with homogeneous Pb isotopic composition (such as NIST glass). A water vapor-assisted method was proposed for non-matrix-matched apatite U-Pb age determination with approximately 4mg/min of water vapor introduced into the laser ablation cell. Apatite U-Pb ages were determined using NIST612 glass as the external standard.

Data and Results: The U-Pb age results of apatite Otter Lake and Durango by calibration against MAD without common lead correction are presented in Fig.2. The initial lead compositions of apatite standards are anchored with the Pb isotopic compositions from Stacey and Kramer's model. The obtained lower intercept ages of Otter Lake and Durango show systemic bias of 2.5% and 6% relative to their reference ages, respectively. The results indicate that significant systematic biases in measured lower intercept ages are observed when calibrating against MAD apatite without common lead correction.

Fig.3 presents the U-Pb results for Otter Lake and Durango, calibrated against apatite MAD after common lead correction using the ^{207}Pb method. The obtained lower intercept age for Otter Lake is less than 1% younger than the reference value. Moreover, the lower intercept age of Durango shows a deviation of −1.7% with the initial lead composition anchored in the Tera-Wasserburg concordia diagram. The results of Otter Lake and Durango using MAD as the external standard with common lead correction via the Tera-Wasserburg plot method are presented in Fig.4. The lower intercept ages of Otter Lake and Durango are 929.0±7.1Ma (2σ, MSWD=1.2) and 29.3±0.5Ma (2σ, MSWD=1.0), showing deviations of 1.7% and 6.6% from their recommended values, respectively. The larger deviation for Durango apatite may be attributed to its higher common lead content and the insufficient spread of the measured Pb/U ratios. Fig.5 shows the U-Pb results of apatite MAD, Otter Lake, and Durango using NIST612 glass as the external standard with the addition of water vapor within the laser ablation cell. The obtained lower intercept ages from the Tera-Wasserburg diagrams for apatite MAD, Otter Lake, and Durango are 474.7±2.7Ma (2σ, MSWD=1.6), 934.8±2.1Ma (2σ, MSWD=2.1), and 31.2±1.2Ma (2σ, MSWD=1.6), respectively. These ages show good consistency with their recommended values within the analytical uncertainties, respectively.

参考文献

[1] Abdullin F, Solé J, Solari L, et al. Single-grain apatite geochemistry of Permian–Triassic granitoids and Mesozoic and Eocene sandstones from Chiapas, Southeast Mexico: Implications for sediment provenance[J]. International Geology Review, 2016, 58(9): 1132−1157.

[2] Krestianinov E, Amelin Y, Neymark L A, et al. U-Pb systematics of uranium-rich apatite from adirondacks: Inferences about regional geological and geochemical evolution, and evaluation of apatite reference materials for *in situ* dating[J]. Chemical Geology, 2021, 581: 120417.

[3] Li Q L, Li X H, Wu F Y, et al. *In-situ* SIMS U-Pb dating of phanerozoic apatite with low U and high common Pb[J]. Gondwana Research, 2012, 21(4): 745−756.

[4] 罗涛, 胡兆初. 激光剥蚀电感耦合等离子体质谱副矿物 U-Th-Pb 定年新进展[J]. 地球科学, 2022, 47(11): 4122−4144.
Luo T, Hu Z C. Recent advances in U-Th-Pb dating of accessory minerals by laser ablation inductively coupled plasma mass spectrometry[J]. Earth Science, 2022, 47(11): 4122−4144.

[5] Pochon A, Poujol M, Gloaguen E, et al. U-Pb LA-ICP-MS dating of apatite in mafic rocks: Evidence for a major magmatic event at the Devonian—Carboniferous boundary in the Armorican Massif (France)[J]. American Mineralogist, 2016, 101(11): 2430−2442.

[6] Morrison J L, Kirkland C L, Fiorentini M, et al. An apatite to unravel petrogenic processes of the Nova-Bollinger Ni-Cu magmatic sulfide deposit, Western Australia[J]. Precambrian Research, 2022, 369: 106524.

[7] Rochín-Bañaga H, Davis D W, Schwennicke T. First U-Pb dating of fossilized soft tissue using a new approach to paleontological chronometry[J]. Geology, 2021, 49(9): 1027−1031.

[8] Rochín-Bañaga H, Davis D W. Insights into U-Th-Pb mobility during diagenesis from laser ablation U-Pb

dating of apatite fossils[J]. Chemical Geology, 2023, 618: 121290.

[9] 罗涛, 卿丽媛, 刘金雨, 等. 激光剥蚀电感耦合等离子体质谱法测定碳酸盐矿物中元素组成[J]. 岩矿测试, 2023, 42(5): 996−1006.
Luo T, Qing L Y, Liu J Y, et al. Accurate determination of elemental contents in carbonate minerals with laser ablation inductively coupled plasma-mass spectrometry[J]. Rock and Mineral Analysis, 2023, 42(5): 996−1006.

[10] Lv N, Bao Z A, Chen K Y, et al. Accurate determination of Cu isotopes in bronze by fsLA-MC-ICP-MS[J]. Atomic Spectroscopy, 2023, 44(6): 418−426.

[11] Liu H, Feng Y, Li M, et al. Further characterization of four natural ilmenite reference materials for *in situ* Fe isotopic analysis[J]. Atomic Spectroscopy, 2023, 44(6): 409−417.

[12] Chew D M, Sylvester P J, Tubrett M N. U-Pb and Th-Pb dating of apatite by LA-ICPMS[J]. Chemical Geology, 2011, 280(1−2): 200−216.

[13] Luo T, Hu Z, Zhang W, et al. Water vapor-assisted "universal" nonmatrix-matched analytical method for the *in situ* U-Pb dating of zircon, monazite, titanite, and xenotime by laser ablation-inductively coupled plasma mass spectrometry[J]. Analytical Chemistry, 2018, 90(15): 9016−9024.

[14] Zhang W, Zhao S, Sun J, et al. Late Mesozoic tectono-thermal history in the south margin of Great Xing'an Range, NE China: Insights from zircon and apatite (U-Th)/He ages[J]. Journal of Earth Science, 2022, 33(1): 36−44.

[15] Chew D M, Spikings R A. Apatite U-Pb thermochronology: A review[J]. Minerals, 2021, 11(10): 1095.

[16] Apen F E, Wall C J, Cottle J M, et al. Apatites for destruction: Reference apatites from Morocco and Brazil for U-Pb petrochronology and Nd and Sr isotope geochemistry[J]. Chemical Geology, 2022, 590: 120689.

[17] Duan L J, Zhang L L, Zhu D C, et al. Apatite MAP-3: A new homogeneous and low common lead natural reference for laser *in situ* U-Pb dating and Nd isotope analysis[J]. Journal of Analytical Atomic Spectrometry, 2023, 38(7): 1478−1493.

[18] Abdullin F, Solari L, Solé J, et al. On LA-ICP-MS U-Pb dating of unetched and etched apatites[J]. Geochronology, 2020, 2020: 1−23.

[19] Lana C, Gonçalves G O, Mazoz A, et al. Assessing the U-Pb, Sm - Nd and Sr - Sr isotopic compositions of the Sumé apatite as a reference material for LA - ICP - MS analysis[J]. Geostandards Geoanalytical Research, 2022, 46(1): 71−95.

[20] Thomson S N, Gehrels G E, Ruiz J, et al. Routine low-damage apatite U-Pb dating using laser ablation-multicollector-ICPMS[J]. Geochemistry, Geophysics, Geosystems, 2012, 13(2): 1−23.

[21] Chew D, Petrus J, Kamber B. U-Pb LA-ICPMS dating using accessory mineral standards with variable common Pb[J]. Chemical Geology, 2014, 363: 185−199.

[22] Storey C, Smith M, Jeffries T. *In situ* LA-ICP-MS U-Pb dating of Metavolcanics of Norrbotten, Sweden: Records of extended geological histories in complex titanite grains[J]. Chemical Geology, 2007, 240(1−2): 163−181.

[23] Hou Z, Xiao Y, Shen J, et al. *In situ* rutile U-Pb dating based on zircon calibration using LA-ICP-MS, geological applications in the Dabie Orogen, China[J]. Journal of Asian Earth Sciences, 2020, 192: 104261.

[24] Luo T, Zhao H, Zhang W, et al. Non-matrix-matched analysis of U-Th-Pb geochronology of Bastnäsite by laser ablation inductively coupled plasma mass spectrometry[J]. Science China: Earth Sciences, 2021, 64(4): 667−676.

[25] Luo T, Deng X, Li J, et al. U-Pb geochronology of wolframite by laser ablation inductively coupled plasma mass spectrometry[J]. Journal of Analytical Atomic Spectrometry, 2019, 34(7): 1439−1446.

[26] Paul A N, Spikings R A, Chew D, et al. The effect of intra-crystal uranium zonation on apatite U-Pb thermochronology: A combined ID-TIMS and LA-MC-ICP-MS study[J]. Geochimica et Cosmochimica Acta, 2019, 251: 15−35.

[27] McDowell F W, McIntosh W C, Farley K A. A precise ^{40}Ar-^{39}Ar reference age for the durango apatite (U-Th)/He and fission-track dating standard[J]. Chemical Geology, 2005, 214(3−4): 249−263.

[28] Thompson J, Meffre S, Maas R, et al. Matrix effects in Pb/U measurements during LA-ICP-MS analysis of the mineral apatite[J]. Journal of Analytical Atomic Spectrometry, 2016, 31(6): 1206−1215.

[29] Jochum K P, Weis U, Stoll B, et al. Determination of reference values for NIST SRM610−617 glasses following ISO guidelines[J]. Geostandards and Geoanalytical Research, 2011, 35(4): 397−429.

[30] Mcfarlane C R M. Allanite U-Pb geochronology by 193nm LA-ICP-MS using NIST610 glass for external calibration[J]. Chemical Geology, 2016, 438: 91−102.

[31] Miyajima Y, Saito A, Kagi H, et al. Incorporation of U, Pb and rare earth elements in calcite through crystallisation from amorphous calcium carbonate: Simple preparation of reference materials for microanalysis[J]. Geostandards Geoanalytical Research, 2021, 45(1): 189−205.

[32] Roberts N M, Rasbury E T, Parrish R R, et al. A calcite reference material for LA-ICP-MS U-Pb geochronology[J]. Geochemistry, Geophysics, Geosystems, 2017, 18(7): 2807−2814.

[33] Paton C, Woodhead J D, Hellstrom J C, et al. Improved laser ablation U-Pb zircon geochronology through robust downhole fractionation correction[J]. Geochemistry, Geophysics, Geosystems, 2010, 11(3): Q0AA06.

[34] Vermeesch P. Isoplot R: A free and open toolbox for geochronology[J]. Geoscience Frontiers, 2018, 9(5): 1479−1493.

[35] Stacey J, Kramers J. Approximation of terrestrial lead isotope evolution by a two-stage model[J]. Earth and Planetary Science Letters, 1975, 26(2): 207−221.

[36] Schaltegger U, Schmitt A, Horstwood M. U-Th-Pb zircon geochronology by ID-TIMS, SIMS, and laser ablation ICP-MS: Recipes, interpretations, and opportunities[J]. Chemical Geology, 2015, 402: 89−110.

[37] 赵令浩, 詹秀春, 曾令森, 等. 磷灰石 LA-ICP-MS U-Pb 定年直接校准方法研究[J]. 岩矿测试, 2022, 41(5): 744−753.
Zhao L H, Zhan X C, Zeng L S, et al. Direct calibration method for LA-HR-ICP-MS apatite U-Pb dating[J]. Rock and Mineral Analysis, 2022, 41(5): 744−753.